

See discussions, stats, and author profiles for this publication at: <https://www.researchgate.net/publication/231629114>

Study of the Polydispersity of Grafted Poly(dimethylsiloxane) Surfaces Using Single-Molecule Atomic Force Microscopy†

ARTICLE *in* THE JOURNAL OF PHYSICAL CHEMISTRY B · FEBRUARY 2001

Impact Factor: 3.3 · DOI: 10.1021/jp0037246

CITATIONS

56

READS

29

6 AUTHORS, INCLUDING:



Boris B Akhremitchev

Florida Institute of Technology

55 PUBLICATIONS 1,241 CITATIONS

SEE PROFILE



Gilbert C. Walker

University of Toronto

172 PUBLICATIONS 4,954 CITATIONS

SEE PROFILE

Study of the Polydispersity of Grafted Poly(dimethylsiloxane) Surfaces Using Single-Molecule Atomic Force Microscopy[†]

Sabah Al-Maawali, Jason E. Bemis, Boris B. Akhremitchev, Rojana Leecharoen, Benjamin G. Janesko, and Gilbert C. Walker*

Department of Chemistry, University of Pittsburgh, Pittsburgh, Pennsylvania 15260

Received: October 10, 2000; In Final Form: November 29, 2000

Single-molecule atomic force microscopy (AFM) was used to study the statistical distribution of contour lengths (polydispersity) of polymer chains grafted to a surface. A poly(dimethylsiloxane) (PDMS) monolayer was grafted on a flat silicon substrate by covalently bonding Cl-terminated PDMS ($M_w = 15000\text{--}20000$) to an OH-silicon surface and characterized using contact angle measurements, ellipsometry, and single-molecule AFM. A model for the single-chain dynamics is presented. The statistical distributions of the polymer contour lengths were found to depend on the concentration of the PDMS polymer used in the grafting solutions. Shifts of the statistical distributions toward higher contour lengths indicated preferential adsorption of longer chains with increasing PDMS:CH₂Cl₂ volume ratios of 0.005–0.16. The gel permeation chromatography (GPC) profile was found to correlate with the most dilute (0.005 volume ratio) AFM data. The polydispersity index (PI) calculated using AFM data was found to be 1.56 compared to 1.62 by GPC. A surface grafted with two PDMS polymer samples of average molecular weights, 3000 and 15000–20000, was found to have a bimodal distribution of contour lengths, with peaks corresponding to the two grafting samples.

Introduction

Man-made polymers synthesized by free radical or polycondensation mechanisms are known to produce a wide distribution of molecular weights and hence characteristic chain lengths.^{1–5} A quantity called the polydispersity index (PI) has been used as a rough guide to understand the distribution of these molecular weights:

$$PI = \bar{M}_w / \bar{M}_n \quad (1)$$

where \bar{M}_w is the weight average molecular weight and \bar{M}_n is the number average molecular weight. A polymer is considered to be monodisperse if PI equals 1. Different analytical methods, such as gel permeation chromatography (GPC) and combinations of light scattering and vapor pressure osmometry, are analytical tools that have been traditionally used to study the distribution of these different molecular weights (polydispersity) of polymers in solution.^{1–4} On the other hand, there are few direct methods for analyzing the lengths of molecules at surfaces.^{1,4} Given the importance of polymer adsorption in technologies ranging from adhesion and lubrication to biology and medicine,¹ new methods for characterizing polydispersity at surfaces are of both practical and fundamental interest.

Single-molecule studies using atomic force microscopy may be able to directly characterize such surface polydispersity, and in this paper we aim to examine that potential. Apart from the usual contact adhesion observed in AFM, polymer distortions can be observed when a grafted polymer chain bridges to the AFM tip^{6–12} as can be seen in Figure 1. The suggestion that this phenomenon could be used to study polymer polydispersity has been suggested by several authors,^{7,8,10b,11} but has not been explored in detail.

In this paper we focus on poly(dimethylsiloxane) (PDMS), mainly because of its widespread importance in industry¹³ and, especially, its value for release applications due to its low surface energy. PDMS's useful bulk properties mainly arise from its unique physical properties of flexibility, low adhesion, and low glass transition temperature. The molecular weight range studied here was, $M_w = 3000$, contour length of 11 nm, as well as $M_w = 15000\text{--}20000$, with contour lengths of $\sim 50\text{--}80$ nm (as calculated using backbone bond lengths of 1.64 Å and bond angles Si–O–Si = 143° and O–Si–O = 110°). The latter one is close to the entanglement molecular weight ($M_w = 18000$) of PDMS.

Experimental Methods

Preparation of Oxidized Silicon.^{14–19} The Si(100) silicon wafers (Siliconquest, CA) were cleaned by heating in a piranha solution (4H₂SO₄:1(30% H₂O₂) (EM Science)) for 10–15 min on a hot plate at approximately 100 °C, and then rinsing in ultrapure water (Millipore). The silicon wafers were next heated in a solution of 1(30% H₂O₂):1HCl:4H₂O for 10 min on a hot plate at approximately 80 °C and then rinsed in ultrapure water. The silicon wafers were next heated again in piranha solution for 10–15 min and rinsed in ultrapure water.

Preparation of Si–OH.^{20,21} Hydroxyls on the silicon surface were obtained by boiling the oxidized silicon wafers for 1 h in ultrapure H₂O (18 MΩ·cm). The silicon wafers were then dried well with argon gas before grafting. It was observed that drying of the Si wafers with inert gas was essential before grafting of PDMS because moisture present in these experiments prevented the grafting reaction from occurring.^{13,21}

Grafting of PDMS of $M_w = 15000\text{--}20000$. Chlorine-terminated PDMS of molecular weight 20000 was used as purchased from Gelest, Inc. The solvent, anhydrous CH₂Cl₂, was used as purchased from Aldrich. Anhydrous pyridine used

[†] Part of the special issue "John T. Yates, Jr. Festschrift".

* To whom correspondence should be addressed.

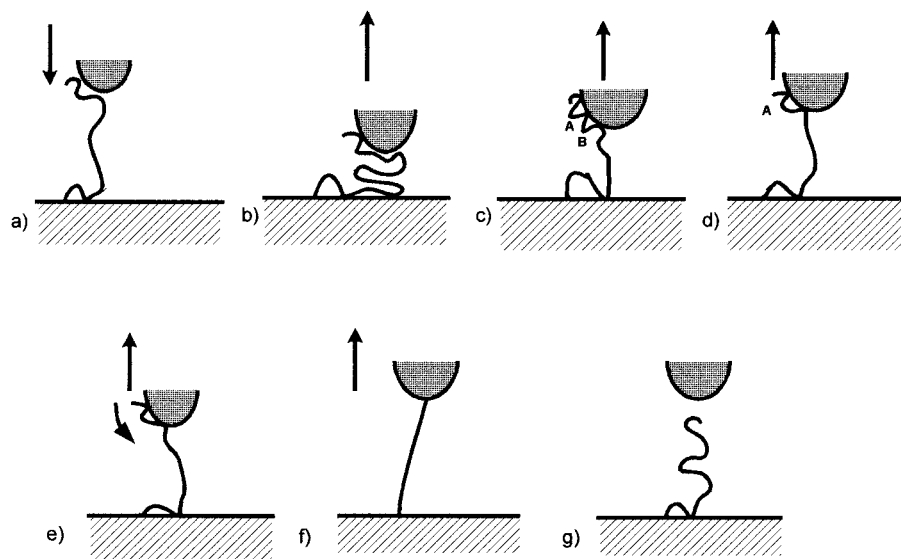


Figure 1. Stages of tip-polymer interaction. (a) Before interaction with the tip, the polymer, grafted to the surface at one end, is in a brush state, again with a small number of monomers on the surface which separate the adsorbed chain into a series of loops and a tail. (b, c) The AFM tip, when it comes into contact with the surface, also creates a collection of contacts with the polymer that lead to a distribution of loops and a tail. Other tip-surface contacts are also formed, whose release may be described by a well-known JKR contact mechanism,²² and are illustrated here. (d, e) The process of separating the tip and surface creates a stress on the polymer chain. This stress is at first released by sliding the polymer chain along one of the surfaces. This causes monomer-surface contacts to collect. (f) At some point of tip separation from the surface, no more stress can be released by such sliding or snakelike motion, and significant stretching of the chain occurs. (g) Finally, complete rupture of the chain from the tip follows, with the sudden rupture of the collected monomer-surface contacts.

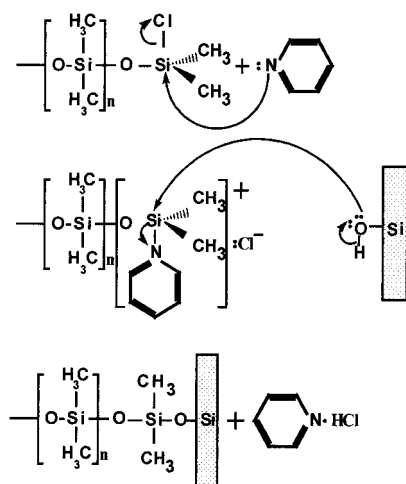


Figure 2. Mechanism for grafting Cl-terminated PDMS on a silicon surface.²¹

as a catalyst in the above reactions^{13,21} was also purchased from Aldrich. Grafting of the silicon surfaces was done in a glovebox. Different polymer surfaces were prepared by changing the PDMS:CH₂Cl₂ volume ratios (0.005, 0.04, 0.11, 0.16) used in grafting. About 20 μ L of pyridine is always added in the reaction as catalyst. The reaction is allowed to occur for approximately 1 h. The reaction mechanism is shown in Figure 2.^{13,21}

Grafting of a Surface Sample Using Two PDMS Polymers of Molecular Weights 3000 and 15000–20000. In one group of samples, OH-silicon surfaces were reacted in dilute solutions of PDMS of molecular weight 3000 (0.02 volume ratio of PDMS:CH₂Cl₂) for 10 min, then rinsed in CH₂Cl₂, and reacted in PDMS solution of molecular weight 15000–20000 (0.11 volume ratio of PDMS:CH₂Cl₂) for 30 min. In the next group of samples, OH-silicon surfaces were in a solution of PDMS, molecular weight 3000, for a longer time of 30 min, then rinsed with CH₂Cl₂, and reacted in a PDMS solution of molecular weight 15000–20000 (0.11 volume ratio of PDMS:CH₂Cl₂).

Cleaning of the Grafted Silicon Surfaces.¹⁴ PDMS-grafted silicon surfaces were washed and sonicated twice with CH₂Cl₂ to remove the physisorbed unreacted PDMS. The surfaces were then washed in 2-propanol (Baker analyzed) and sonicated for about 10 min. They were then washed in a solution of dodecyl sulfate (Boehringer Mannheim) and rinsed in deionized water several times.

Contact Angle Measurements.²² Contact angle measurements of the Si-OH and Si-PDMS surfaces with ultrapure water were studied using a custom-made contact angle apparatus equipped with a video camera. With this apparatus advancing contact angles can be measured with $\pm 3^\circ$ accuracy.

Ellipsometry. In this work, a single-wavelength null ellipsometer, model L117 made by Gaertner Scientific Corp., was used to measure the film thickness of PDMS ($M_w = 15000$ – 20000) of different PDMS:CH₂Cl₂ volume ratios. The measurements were done at a 70° angle of incidence with a He-Ne laser of wavelength 6328 Å as a light source. The measurements were done for the bare silicon wafers and the PDMS-grafted silicon surfaces.^{23–25} The readings were done within 16 h of preparation of the samples since it was observed that the monolayers deteriorated after 40 h when they were stored in deionized water.

AFM Methods. AFM experiments were performed using a Digital Instruments multimode AFM equipped with a Nanoscope IIIa controller and a fluid cell. For the experiments, silicon cantilevers, CSCS12 Contact Ultrasharp, were purchased from Silicon MDT Ltd. The spring constants used to calculate the forces were directly taken from the manufacturer's specifications and are expected to have 25% uncertainty. To avoid capillary forces between an AFM tip and a sample, the force measurements were performed under a 25 mM NaCl solution (Aldrich) freshly prepared with ultrapure water (18 M Ω ·cm).^{22,26} The experiments were performed in force mode, collecting laterally resolved force plots. An extensive statistical analysis of the lengths of polymer elongations was achieved by using custom software to analyze a high number (>1000) of data samples

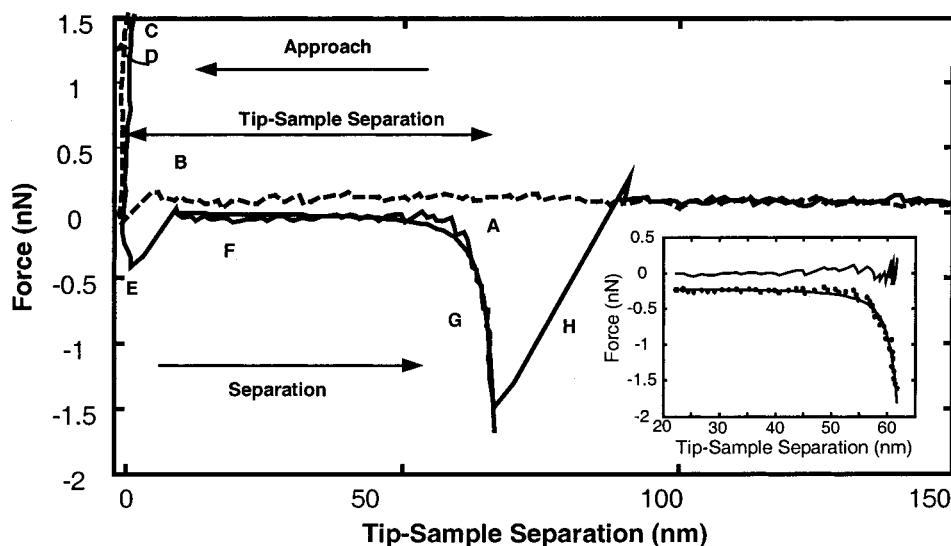


Figure 3. Typical force vs distance plot obtained for a surface with PDMS polymers grafted at the surface. Approach: A, no AFM tip–sample interaction; B, jump to contact; C and D, repulsive contact with the surface under increasing (C) and decreasing (D) force. Separation: E, attractive force due to surface adhesion; F, polymer sliding off the tip; G, an attractive force due to polymer stretching; H, the polymer chain ruptures from the AFM tip. Inset: hybrid model fit to the data (the solid line) providing a persistence length of 0.28 nm. The error between the data and the fitted values is indicated by the line above the fitted data.

TABLE 1: Ellipsometry Parameters Obtained at Different PDMS:CH₂Cl₂ Ratios for $M_w = 15000$ – 20000 PDMS

sample	Ψ (deg)	Δ (deg)	d (nm)
blank Si (100)	10.3 ± 0.1	175 ± 2	0.55 ± 0.3
0.005 volume ratio	10.5 ± 0.1	157 ± 3.3	3.56 ± 0.4
0.04 volume ratio	11.6 ± 0.2	152 ± 3.0	5.01 ± 0.37
0.11 volume ratio	11.1 ± 0.2	145.8 ± 2.5	5.88 ± 0.34
0.16 volume ratio	11.4 ± 0.2	147.9 ± 2.6	5.65 ± 0.25

similar to that data shown in Figure 3. The contour lengths and persistence lengths of the polymer chains and force interactions were obtained according to models described below.

Results and Discussion

Characterization of the Surface Grafted with Monolayers.

Contact Angle Results. SiOH surfaces were found to have contact angles of $\sim 67^\circ$. The advancing contact angles for grafted PDMS surfaces are found to be 106 – 109° , which are within the expected range of values for PDMS.¹³

Ellipsometry Results. In ellipsometry, p- and s-polarized light incident on a surface reflect with associated changes in the phase and amplitude of the outgoing E_p and E_s components (therefore producing an elliptical light wave). These phase and amplitude differences of p- and s-polarizations are given by Fresnel reflection coefficients R_p and R_s . Ellipsometry analyzes the ratios of these R_p and R_s coefficients, i.e., the relative phase change, Δ , and the relative amplitude change, $\tan \Psi$. One can relate Δ and Ψ to the thickness of a film or a monolayer at the surface by equations given by Azzam and Bashara.²³ In this work, the model used to calculate the thickness of the monolayers was a single-film model,^{23,24} 0–1 (air–PDMS) and 1–2 (PDMS–silicon) interfaces. It was assumed that the ambient air has refractive index n_0 (1), the monolayer has refractive index n_1 (1.43 for PDMS),²⁷ and the silicon substrate has refractive index n_2 ($3.875 - 0.018j$).

Table 1 gives the thickness of monolayers generated using different PDMS:CH₂Cl₂ volume ratios, as obtained via ellipsometry. The thickness of a monolayer is shown to increase from ~ 35 to 60 Å in the first three PDMS:CH₂Cl₂ volume ratios and then drops slightly at the highest value measured. If we assume the coverage to be uniform, these thicknesses are

consistent with surface structures of terminally attached chains that are approximately in brush forms, with few nongrafted polymer contacts to the surface.²⁸ The radius of gyration of the $M_w = 15000$ – 20000 PDMS polymers free in solution would be 15 – 17 Å,²⁹ which is about half the predicted extension of a mushroom of similar chemical composition but in a good solvent extending from the surface;^{28,30} in the studies reported here, of course, there is covalent grafting of one end of the chain and the solvent quality is poor, and thus these characteristic lengths are given simply for comparison.

AFM Results. Theoretical Model for AFM Results. In our AFM stretching experiments we describe five major stages of polymer adsorption dynamics, as illustrated in Figure 1. (a) Before interaction with the tip, the polymer, grafted to the surface at one end, is in a brush state, again with a small number of monomers on the surface which separate the adsorbed chain into a series of loops and a tail. (b, c) The AFM tip, when it comes into contact with the surface also creates a collection of contacts with the polymer that lead to a distribution of loops and a tail. In the compression, other tip–surface contacts are also formed, whose subsequent release may be described by a well-known JKR model of adhesion,²² and are not of central interest here. (d, e) The process of separating the tip and surface creates a stress on the polymer chain. This stress is at first released by sliding the polymer chain along one of the surfaces, as described below. (f) At some point of tip separation from the surface, no more stress can be released by such sliding or snakelike motion, and significant stretching of the chain occurs. (g) Finally, complete rupture of the chain from the tip follows. A force plot illustrating most of these stages may be seen in Figure 3.

Model for Polymer Dynamics on the Tip. We use the model of Sevick and co-workers.³¹ We assume that the linear polymer chain is composed of monomers of size l that bind to a surface with a contact energy of $\epsilon k_B T$ each. These contacts divide the chain into a series of loops and tail(s). For chains longer than ca. 40 monomers, the number of monomers in a tail is proportional to the total number of monomers of the entire polymer.¹ If an extended portion of the chain is pulled, then the resulting tension is transmitted to the nearest monomer–

surface contacts. If we make the simplifying assumption that the surface–monomer potential energy function along the path of attachment is $U(r)$, with barrier height h , width w , and depth ϵ , then the applied tension, f , will reduce $U(r)$ by fr . There are two limits of expected force profiles, depending on the rate of pulling. In one case, the tip extension rate is fast relative to the activation kinetics of detachment; the surface-bound monomer has insufficient time to escape the barrier to attachment even though the barrier is continually being reduced by tension. In this limit the detachment occurs at a large extensional force that reduces the barrier to zero. In the case of slow tip motion, which is relevant for our data, the rate of extension of a pulled tether to the polymer chain is sufficiently slow that monomer–surface contacts can detach and re-form many times (10^8 s^{-1}) over the time scale of tip motion over a similar distance.

This latter case is predicted to lead to a force that indicates only averaged information about the strength of the monomer surface contacts, and is, in fact, a constant force.³¹ Assuming that the chain is Gaussian, the minimized free energy (in units of $k_B T$) of an absorbed chain with a tether of N monomers extended a distance r from the surface is $F \approx \epsilon(w/l) - N\epsilon^2/4$. The slow extensional force is $f = \partial F/\partial r \approx \epsilon k_B T/l$. Moreover, under the tension, nearest-neighbor monomers can exchange at one surface binding site, or at a somewhat different energy cost, a monomer could move to a neighboring surface site. This constant force is reminiscent of pulling the chain through a viscous medium.

Model for Nonlinear Extension of the Chain. The extension of the chain can cause non-Gaussian distributions of its end-to-end length. We calculate the forces required to generate such conformations using the wormlike chain (WLC) model. This model describes a polymer chain as consisting of N bonds with fixed lengths l joined in a linear succession. The WLC model maintains the angles at the bond junctions fixed, but the dihedral angles are free to rotate.^{8,9,10a,12,32} The elastic restoring force of the polymer chain, F_{chain} (nN), is calculated as follows:

$$F_{\text{chain}} = \frac{k_B T}{p} \left(\frac{1}{4(1 - r/L_{\text{contour}})^2} - \frac{1}{4} + \frac{r}{L_{\text{contour}}} \right) \quad (2)$$

where r (nm) is the end-to-end distance of the polymer chain, k_B is the Boltzmann constant, T is the temperature, p is the persistence length (nm), and L_{contour} is the contour length (nm) of the polymer chain.

A hybrid model combining these two processes, (i) activated monomer–surface ruptures in the slow tip motion limit, giving constant forces, and (ii) extensions of the chain, leading to nonlinear forces, is incorporated in the fits to the data, as illustrated in Figure 3. We have analyzed 300+ force plots similar to that shown in Figure 3. The persistence lengths were found to have an average value of 0.31 nm, which is close to the expected value for a single PDMS chain free in solution, 0.25 nm.³³ The distribution of persistence lengths can be further decomposed into two distributions peaked at 0.11 ± 0.16 and 0.31 ± 0.14 nm. Thus, we infer that we typically study the force–distance profile of a single chain at a surface.

Figure 4 shows a case where multiple sliding events occur to reduce stress at low extension, and when the first polymer loop is taken up, only one contact point remains to slide. The constant force we obtain from the fits is about 140 pN. This corresponds to a monomer–surface binding energy of ca. $4 \times 10^{-20} \text{ J}$ (assuming a monomer length of 0.28 nm), which is a reasonable value given the simplicity of the above model. The persistence length, 0.13 nm, obtained from fits of the WLC force

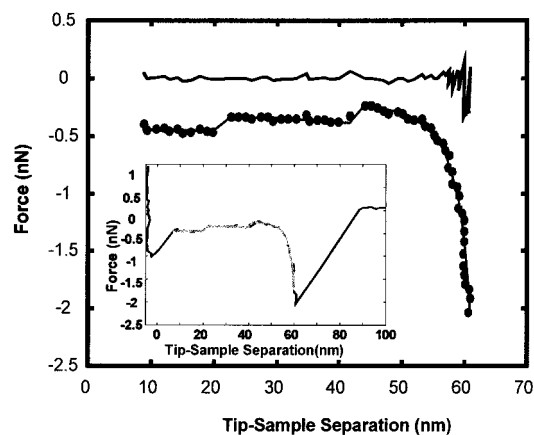


Figure 4. Force plot with a primary adhesion and a secondary adhesion due to PDMS stretching. The flat, steplike profile is caused by the chain sliding on the tip, as described in the text. The persistence length obtained from fitting the hybrid model is 0.13 nm, suggesting that, unlike in Figure 3, a loop is being stretched. The error between the data and the fitted values is indicated by the line above the fitted data. The inset shows the entire force plot.

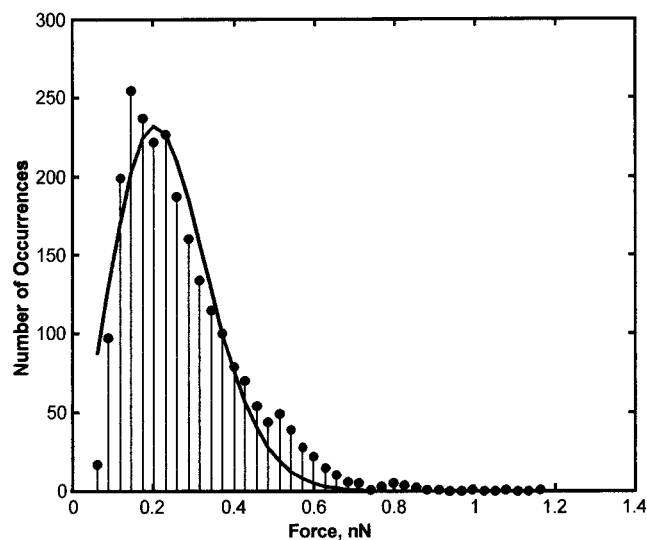


Figure 5. Statistical distribution of polymer stretching rupture forces observed between the AFM tip and the PDMS monolayer at the surface.

model is half that obtained from fits to data such as in Figure 3. This suggests that a loop (or two parallel chains)¹² is being stretched in Figure 4 and a tail in Figure 3.

Magnitudes of Final Rupture Forces. The magnitudes of final rupture forces in our case study were within the range of 0.1–2 nN as shown in Figure 5. Due to the uncertainty in the manufacturer’s spring constants, the error of force calculations is expected to be $\pm 25\%$. The detection limit of force determination was approximately 0.1 nN. The statistical distribution when fitted to a Poisson distribution function (solid black line, with an error of 19%) shows 0.62 nN to be the most probable force and the lowest force to be 0.12 nN.³⁴ The magnitude of the force is low, indicating that the polymer–tip surface contacts are not covalent. If we were breaking such bonds, which we are not, the rupture forces would be much larger, e.g., Si–O (9.7 nN) and Si–Si (2.9 nN).^{35–38} If one were to assume that 0.12 nN is the rupture force of one noncovalent contact following the method shown by Beebe et al.,²⁶ then the most probable number of polymer–tip contacts being broken at rupture would be ~ 5 .

Distribution of the Contour Lengths. Figure 6 shows the statistical distribution of polymer chain contour lengths obtained

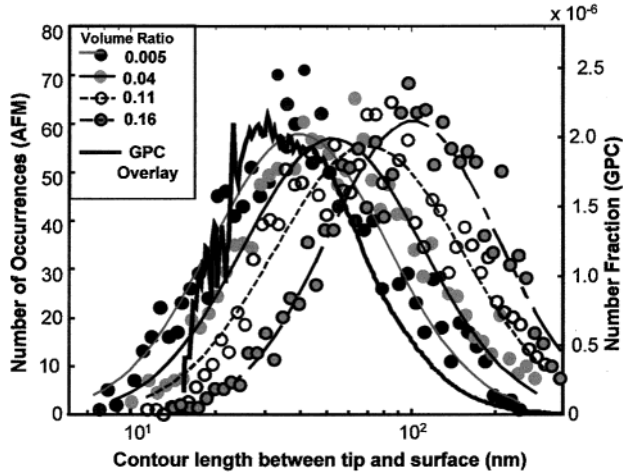


Figure 6. GPC profile overlaid with the AFM statistical distributions of contour length between the tip and surface for different PDMS:CH₂Cl₂ volume ratios indicated in the plot. See the text for further explanation.

TABLE 2: Calculated Peak Heights and Peak Widths at Different PDMS:CH₂Cl₂ Volume Ratios for $M_w = 15000$ – 20000 PDMS

PDMS vol ratio in CH ₂ Cl ₂	peak position at the highest probability calcd using Gaussian fits (nm)	peak width using Gaussian fits (nm)	PI
0.005	40.0	63.2	1.56
0.04	52.7	85.4	1.56
0.11	69.9	119.7	1.47
0.16	101.0	152.7	1.4

with increasing volume ratios of PDMS to CH₂Cl₂ from 0.005 to 0.16. The GPC results are also shown. The x axis, chain contour lengths at the attachment with the AFM tip (nm), is plotted on the logarithmic scale, and the y axis is the number of occurrences per number fraction. These statistical distributions have been corrected to account for rupture of contact adhesion, which can obscure single-molecule data at small tip–sample separations.³⁹ The statistical distributions of chain lengths plotted on the logarithmic scale are well fit by Gaussian distribution functions⁴ with errors of $\sim 10\%$. In GPC the log of molecular weight goes as the volume eluted. From the correspondence of the chain length obtained from the AFM and GPC experiments, we conclude that in the AFM experiment the chain tends to slide to its end, with a bunching of multiple monomer contacts. As the polymer chain is stretched, the physisorbed chains and loops slide across the surfaces until, at the end of the chain or surface, a critical number of monomers are collected, which no longer slide across the surface. It is the sudden loss of this collection of monomer contacts that is represented in the final rupture force. This is shown schematically in Figure 1 and is explained further within the caption. In this model the shape is convolved within the measured length distribution because because polymer chain absorption ruptures, prior to the collection of monomers at the end of the chain, shift the measured distributions to lower average lengths, as well as increase the measured polydispersity. We find good correlation between the dilute (0.005 volume ratio) and the GPC data, and consequently presume that the tip shape convolution plays a minor role.

Figure 6 also shows that the average contour length increases with CH₂Cl₂ volume ratio. Table 2 shows that the peak width also increases with higher volume ratio, indicating a wider distribution of lengths at the surface. It can thus be inferred from Table 2 that there is preferential adsorption and reaction

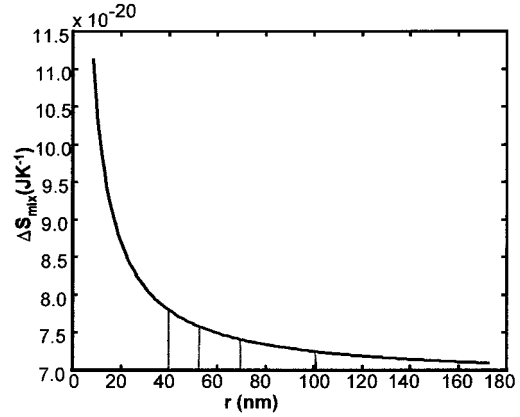


Figure 7. Decrease of entropy of mixing with an increase in polymer chain lengths using Flory–Huggins theory.¹ The lines indicate the peak positions of experimental distributions of contour lengths obtained at different PDMS:CH₂Cl₂ volume ratios (see Figure 8).

of long chains or high molecular weight polymers at higher concentrations. This AFM-based observation is consistent with earlier studies using other techniques that studied the remaining unreacted solution. In these studies, the central observation was that high molecular weight polymers adsorb on the surface preferentially over low molecular weight polymers at equilibrium.^{1–5} This observation is explained qualitatively in Figure 7, which shows the entropy of mixing vs chain length. Longer chains are likely to fall out of solution since their mixing entropy per mass is lower, and shorter chains will prefer to stay in solution because their mixing entropy is higher. Note that there are three expected regimes of molecular weight distribution depending on grafting solution concentration. In the first the concentration of polymers in the solution is so small that all chains have equal probability of finding binding sites. In the second, surface saturation is being approached and binding becomes preferential; only the higher molecular weight fraction is entirely bound, whereas smaller molecules have access only to sites not occupied by the big ones. In the third regime, all sites have been taken, and the surface polydispersity becomes independent of grafting solution concentration. Our data indicate that over the concentration range we studied the second regime was explored.

Using AFM results of contour lengths (L_i), we convert them to molecular weights using the following equation:

$$M_i = \frac{74L_i}{0.28 \text{ nm}} \quad (3)$$

Here, 74 is the molecular weight of one siloxane monomer and 0.28 nm is the length of one monomer. Average M_n and M_w are calculated as follows:

$$\bar{M}_n = \frac{1}{N} \sum M_i \quad (4)$$

$$\bar{M}_w = \frac{\sum M_i^2}{\sum M_i} \quad (5)$$

The PI index is calculated as eq 1; values are given in Table 2. The PI found by the AFM stretching experiment is close to the value obtained from the GPC solution measurement (1.62) for the lower volume ratio surfaces.

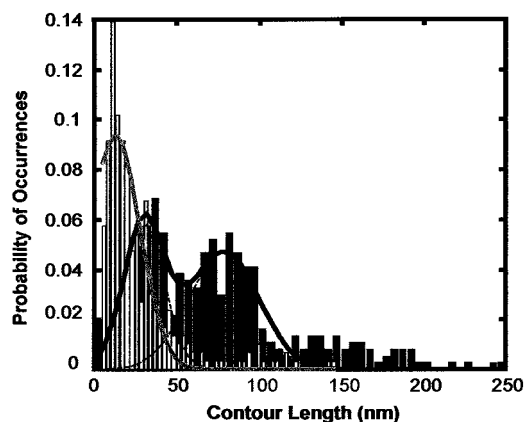


Figure 8. Contour lengths vs normalized number of occurrences. The black bars show data for a sample surface of mixed PDMS, average molecular weights 3000 and 15000–20000. The gray bars show data for a sample surface prepared using PDMS of average molecular weight 3000. The solid black line is a sum of two Gaussians for the data for a surface prepared with both the $M_w = 3000$ and $M_w = 15000$ –20000 samples; the peak positions correspond to 28 and 83 nm. The gray line is a Gaussian fit to the surface made of PDMS of average molecular weight 3000 alone, and the peak position is 20 nm. See comments in the text.

Analysis of Surfaces Grafted Using Two PDMS Samples of Different Average Molecular Weights. Figure 8 shows the distribution of contour lengths of polymers on a surface grafted using two fractions of PDMS of different average molecular weights, 3000 and 15000–20000 (black bars), and a distribution of chain contour lengths on a surface prepared using only PDMS of molecular weight 3000 (gray bars). A bimodal statistical distribution of contour lengths is obtained for a surface grafted using two PDMS compounds of different molecular weights. The first peak position is about ~ 28 nm, and the second peak position is ~ 83 nm, using the sum of the two Gaussian fits. The peak position for PDMS of molecular weight 3000 might be expected to be ~ 11 nm; it is possible that tip jump following the rupture of the primary force of adhesion (JKR adhesion force) may partially obscure single-chain data for the shortest chains. Further study of this convolution will probably be required for higher resolution of surface polymer polydispersity measurements. The second peak (~ 83 nm) is close to the expected contour length (50–80 nm for $M_w = 15000$ –20000) for the higher molecular weight PDMS. The surface prepared using only PDMS of molecular weight 3000 (gray bars) in Figure 8 gives a peak at about 15 nm, which is close to the expected contour length for $M_w = 3000$ PDMS, although a Gaussian function would fit well only the long contour lengths, as seen in Figure 8. Figure 9 shows the same bimodal distribution (black bars) as in Figure 8 as well as a second distribution. The second distribution was obtained from a sample surface prepared using the same two PDMS compounds of $M_w = 3000$ and 15000–20000. Here the OH–silicon surface was allowed to react for a longer time (30 min) in the PDMS of molecular weight 3000. It can be seen from Figure 9 that the second peak of 83 nm observed in Figure 8 (black bars) is reduced, indicating there were few sites left to react with the PDMS of higher molecular weight and most of the sites at the surface had already reacted with the PDMS of molecular weight 3000. The distributions shown in Figures 8 and 9 are not corrected for the adhesion jump off. The correction for these distributions was small enough to ignore. If they had been corrected, the small contour length peak positions would be shifted to lower values by no more than 10%.

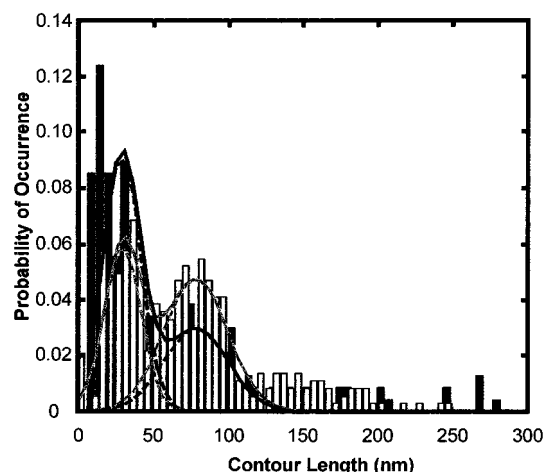


Figure 9. Contour lengths vs normalized number of occurrences. Both of the overlaid plots (open bars and black bars) show sample surfaces prepared from mixed PDMS compounds, average molecular weights 3000 and 15000–20000. Open bars are results for a surface that was allowed to react for 10 min in PDMS, average molecular weight 3000, and then reacted in PDMS of average molecular weight 15000–20000 for 30 min. The black bars show length distributions for a surface that was allowed to react for 30 min in PDMS of molecular weight 3000 and 30 min in PDMS of molecular weight 15000–20000.

Conclusions

It has been shown that there is significant potential for AFM to analyze contour lengths of polymers/macromolecules at surfaces. The values of persistence lengths and other parameters obtained from fitting the force–distance profiles indicate that the measurements typically involved stretching single PDMS molecules grafted to the underlying surface. The generality of this technique will presumably depend on the type of polymer, film, and AFM tip used.

Acknowledgment. We gratefully acknowledge the Office of Naval Research (Grant ONR-N00014-96-1-0735), National Science Foundation (Grant NSF-9816820), and DARPA (Grant DAAD16-99-C-1036) for financial support. G.C.W. thanks 3M Co. for an Untenured Faculty Award. S.A.-M. thanks the Islamic Development Bank and the Government of Sultanate of Oman for predoctoral fellowships. R.L. and B.B.A. thank the Mellon Foundation for predoctoral fellowships.

References and Notes

- (1) Fleer, G. J.; Stuart, M. A. C.; Scheutjens, J. M. H. M.; Cisgrove, T.; Vincent, B. *Polymers at Interfaces*; Chapman & Hall: London, New York, 1993.
- (2) Stuart, M. A. C.; Scheutjens, J. M. H. M.; Fleer, G. J. *J. Polym. Sci.* **1980**, *18*, 559.
- (3) Fleer, G. J.; Scheutjens, J. M. H. M.; Stuart, M. A. C. *Colloids Surf.* **1988**, *31*, 1.
- (4) Cooper, A. R. *Determination of Molecular weight*; John Wiley and Sons: New York, 1989; Chapter 10.
- (5) Dobias, B. *Coagulation and Flocculation, Theory and Applications*; Marcel Dekker: New York, 1993.
- (6) Bustamante, C. *Science* **1994**, *265*, 1599.
- (7) Ikai, A. *Surf. Sci. Rep.* **1996**, *26*, 261.
- (8) Ortiz, C.; Hadziioannou, G. *Macromolecules* **1999**, *32*, 780.
- (9) Li, H.; Rief, M.; Oesterhelt, F.; Gaub, H. *Adv. Mater.* **1998**, *3*, 316.
- (10) (a) Rief, M.; Fernandez, J. M.; Gaub, H. *Phys. Rev. Lett.* **1998**, *81*, 4764. (b) Florin, E. L.; Moy, V. T.; Gaub, H. E. *Science* **1994**, *264*, 415.
- (11) (a) Li, H.; Liu, B.; Zhang, X.; Gao, C.; Shen, J.; Zou, G. *Langmuir* **1999**, *15*, 2120. (b) Yamamoto, S.; Tsujii, Y.; Fukuda, T. *Macromolecules* **2000**, *33*, 5995–5998.

- (12) Bemis, J. E.; Akhremitchev, B. B.; Walker, G. C. *Langmuir* **1999**, *15*, 2799.
- (13) Clarson, S. J.; Semlyen, J. A. *Siloxane Polymers*; Prentice Hall: Englewood Cliffs, NJ, 1993.
- (14) Luo, H.; Chidsey, C. E. D. *Appl. Phys. Lett.* **1998**, *72*, 477.
- (15) Linford, M. R.; Fenter, P.; Eisenberger, P. M.; Chidsey, C. E. D. *J. Am. Chem. Soc.* **1995**, *117*, 3145.
- (16) Wade, C. P.; Chidsey, C. E. D. *Appl. Phys. Lett.* **1997**, *71*, 1679.
- (17) Higashi, G. S.; Becker, R. S.; Chabal, Y. J.; Becker, A. J. *Appl. Phys. Lett.* **1991**, *58*, 1656.
- (18) Allongue, P.; Kiellling, V.; Gerisher, H. G. *Electrochim. Acta* **1995**, *40*, 1353.
- (19) Le Grange, J. D.; Markham, J. L.; Kurkjian, C. R. *Langmuir* **1993**, *9*, 1749.
- (20) Bouhacina, T.; Michel, D.; Aime, J. P.; Gauthier, S. *J. Appl. Phys.* **1997**, *82*, 3652.
- (21) Rubinsztajn, S.; Cypryk, M.; Chojnowski, J. *J. Organomet. Chem.* **1989**, *367*, 27.
- (22) Israelachvili, J. *Intermolecular and Surface Forces*, 2nd ed.; Academic Press: New York, 1991.
- (23) Azzam, R. M. A.; Bashara, N. M. *Ellipsometry and Polarized Light*; North-Holland Publishing Co.: Amsterdam, 1977.
- (24) Wasserman, S. R.; Whitesides, G. M.; Tidswell, I. M.; Ocko, B. M.; Pershan, P. S.; Axe, J. D. *J. Am. Chem. Soc.* **1989**, *111*, 5852.
- (25) Tompkins, H. G. *A User's Guide to ELLIPSOMETRY*; Academic Press: New York, 1993.
- (26) Wenzler, L. A.; Moyes, G. L.; Olson, L. G.; Harris, J. M.; Beebe, T. P., Jr. *Anal. Chem.* **1997**, *69*, 285.
- (27) Brandrup, J.; Immergut, E. H. *Polymer Handbook*; Wiley: New York, 1989; Vol. VII/464.
- (28) De Gennes, P. G. *J. Chim. Phys. (Paris)* **1976**, *37*, 1443.
- (29) The unperturbed radius of gyration, R_g , is given by $R_g = l n^{1/2} / 6^{1/2} = l (M_w / M_{w0})^{1/2} / 6^{1/2}$, where n is the number of segments, l is the effective segment length, M_w is the molecular weight of the polymer, and M_{w0} is the segment molecular weight.²²
- (30) Alexander, S. *J. Chim. Phys. (Paris)* **1977**, *38*, 983.
- (31) Haupt, B. J.; Ennis, J.; Seveck, E. M. *Langmuir* **1999**, *15*, 3886.
- (32) (a) Flory, P. J. *Statistical Mechanics of Chain Molecules*; Hanser Publishers: Cincinnati, 1988. (b) Flory, J. *Principles of Polymer Chemistry*; Cornell University Press: Ithaca, NY, 1995.
- (33) Sendon, T. J.; di Meglio, J.-M.; Auroy, P. *Eur. Phys. J. B* **1998**, *36*, 211.
- (34) Note: Effect of cleaning the AFM silicon tip by argon plasma etching. After the AFM silicon tips were cleaned for 2 min using argon plasma, the rupture forces were observed to increase from 0.62 nN observed earlier in Figure 5 to 1.2 nN. Ghatak et al. (Ghatak, A.; Vorvolakos, She, K. H.; Malotky, D. L.; Chaudhury, M. K. *J. Phys. Chem. B* **2000**, *104*, 4018) also observed this effect.
- (35) Nguyen, Q.; Kausch, H. H. *Colloid Polym. Sci.* **1991**, *269*, 1099.
- (36) Kausch, H. H. *Polymer Fracture*, 2nd ed.; Springer-Verlag: Berlin, New York, 1987.
- (37) Atkins, P. W. *Physical Chemistry*, 4th ed.; W. H. Freeman and Co.: New York, 1990.
- (38) A calculation of forces that are required to rupture covalent bonds based on Morse potentials shows that Si-O/Si-Si rupture forces are much higher than the forces we observe (0.1–1.2 nN). The magnitude of the bond rupture force F_b is predicted from the binding (dissociation) energy D_e using the Morse potential, $V = D_e(1 - e^{-a(r-r_e)})^2$. r_e is the equilibrium bond length, and a is a parameter controlling the width of the potential well. Where $x = r - r_e$, the force is given by $F = -\partial V / \partial x = 2aD_e(e^{-ax} - e^{-2ax})$ and the maximum force can be calculated as $\partial^2 V / \partial x^2 = 0 = -2D_e a^2 e^{-ax} + 4D_e a^2 e^{-2ax}$. If we solve for x , we obtain $x = (\ln 2)/a$, and if we substitute x into the first equation of force, we obtain $F_b = (1/2)D_e a$.
- (39) From the distribution of the adhesion jump off events, as a function of deflection in units of nanometers, the probability of an adhesion jump with respect to distance is obtained. The contour length is then divided by this probability, $P_{ci} = P_i / \langle \Delta v \rangle \sum_j \langle \Delta l_w \rangle \Delta d_j$. Here P_{ci} is the corrected probability of an event at contour length i , P_i is the uncorrected probability of an event at that contour length obtained from our experiment, and Δd_j is the experimentally observed probability of an adhesion jump off of deflection i . The reasoning for the above equation is that if at a given length half the time there is an adhesion jump obscuring the detection of polymer stretching, then the probability of a polymer stretching event should be twice as high as we detect at that distance.